

Modelling Perimeter Heating Demand:
A Function Of Occupant Thermal Comfort



KPMB LAB

Introduction & Background

As the focus of high performance building design expands from a focus on mechanical systems to include a focus on envelope design, it is useful for architectural designers to be able to understand the performance characteristics of various facade configurations at an early stage of design.

Indeed, emerging regulatory requirements for high performance buildings often require guarantees of overall building performance, thermal energy demands, etc. at early stages of design (e.g. conclusion of schematic design phase.) Moreover, it is increasingly important for architects to be able to understand the impact of facade design decisions on occupant thermal comfort, quality of daylighting, etc. at an early stage, when it is easiest to align the building massing, plan, section, envelope strategies, etc. to produce optimal outcomes.

Occupant thermal comfort is influenced by the indoor air temperature, mean radiant temperature, solar radiation, air velocity and humidity. Accurate modelling of these parameters requires knowledge of the mechanical systems used, internal heat gains, and the thermal conductance and capacitance of surrounding materials (Berardi and Soudian

2019). This information is typically unavailable during schematic design phase, which signals the need for simplified thermal comfort models.

A handful of tools have the ability to evaluate indoor thermal comfort using the limited information available during early stages of design (Hoyt 2016, Menchaca-Brandan, et al. 2017). These tools require basic information about the indoor and outdoor environmental conditions, the glazing geometry, and the target window U-value. These inputs are easily obtainable during schematic design. However, most of these tools assume the absence of perimeter heating. This muddles potential arguments that higher performance facades result in better thermal comfort, because a properly designed perimeter heating system should inevitably compensate for facade-induced discomforts (Berglund, Yoshino and Kuno 1997).



Residential suite with relatively equal weighting of solid façade and punched windows.

Despite this logical gap in efforts to link facade performance to indoor thermal comfort during early stages of design, it is clear that a lower performance facade should require more heating energy to maintain an acceptable level of comfort. The exact quantity of this energy, if it could be isolated, would be descriptive of both facade performance and indoor thermal comfort.

This paper aims to demonstrate how thermal comfort and energy quantities can be brought into discussions about facade performance during early stages of design. This is achieved through a novel approach wherein the perimeter heating energy demand is treated as the energy required to deliver thermally comfortable conditions. A purpose-built Python model is

introduced and tested using an archetypal Toronto residential suite as an example. The results of heating energy demand, peak heating demand and peak radiant panel temperature are reported. Lastly, intricacies and limitations of the modelling approach are discussed.

Methods

Experiment Overview

A model was developed to quantify the heating energy required to maintain thermal comfort in an archetypal residential suite in Toronto, Ontario. To minimize the number of inputs, the model operates under a strict set of assumptions. The archetypal suite has one exterior wall with one window and thermal

comfort is calculated for an occupant position 2 m from the midpoint of this window and 1.2 m above the floor (Figure 1). Heat is delivered to the space via a radiant ceiling panel alongside the window opening. The depth of the panel is 24 inches.

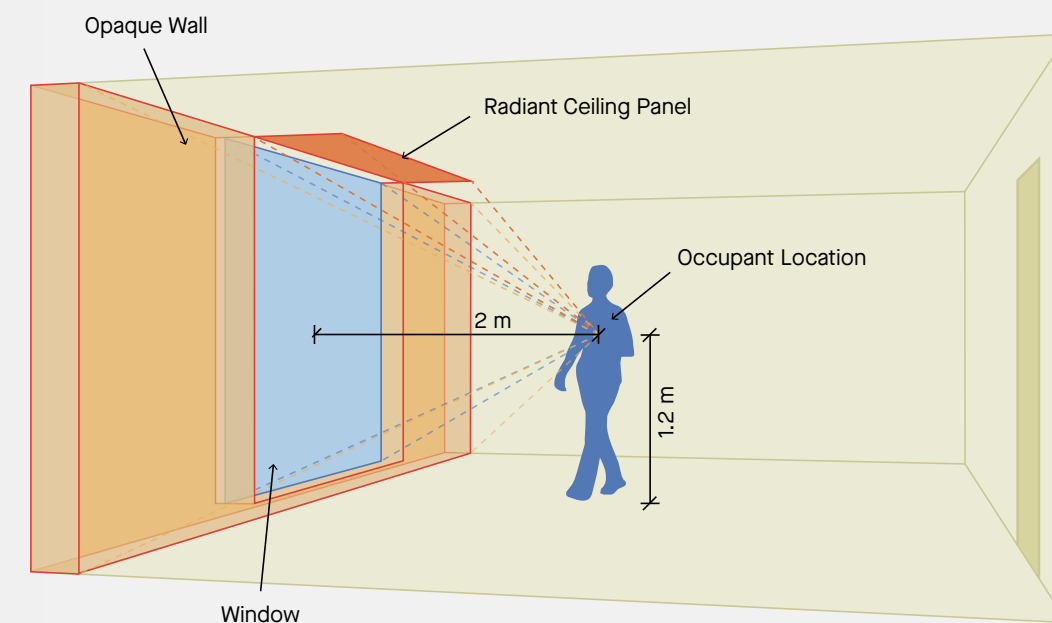


Figure 1 – Schematic representation of the experiment. Dashed lines represent the view factors to the respective surfaces. The floor, ceiling and interior walls are assumed to be the same temperature as the indoor air.

The model was built using the programming language Python (version 3.8.8). Several third-party Python libraries contributed to the workflows, including ladybug-geometry (Sadeghipour Roudsari and Pak 2013), pvlib (Holmgren, Hansen and Mikofski 2018) and pythermalcomfort (Tartarini and Schiavon 2020). The model has no graphical user interface (GUI). Instead, the user provides an Excel sheet containing the inputs. The model uses annual hourly weather data as outdoor boundary conditions. For this particular experiment, the CWEC (Canadian Weather for Energy Calculation) file for Toronto International Airport was applied. The file consists of 12 typical months' worth of observations selected from the years 1998-2017 (Environment Climate Change Canada 2020).

To assess the model's ability to evaluate early-stage design decisions, three facade types of varying window U-value, wall U-value and SHGC (solar heat gain coefficient) were simulated (Table 1). The facade types, which correspond to Low Performance, Average Performance and High Performance, are adapted from a previous study considering Toronto-area MURBs (multi-unit residential buildings) (Ozkan, et al. 2018). In addition, a 40% window-to-wall ratio (WWR) and 80% WWR version of each facade type was tested. Also, 4 compass orientations were considered. In total 24 scenarios were simulated.

	LOW PERFORMANCE	AVERAGE PERFORMANCE	HIGH PERFORMANCE
Wall U-value (W/m ² K)	0.247	0.21	0.18
Glazing U-value (W/m ² K)	2.5	1.7	1
Glazing SHGC	0.45	0.35	0.25
Glazing T _{sol}	0.36	0.28	0.2
WWR (%)		40, 80	
Orientation		North, East, South, West	

Table 1 – The facade types simulated.

Model Description

The most important output of the model is the amount of heat energy (kWh) required to maintain thermally comfortable conditions for the assumed occupant location. To produce this output, it is necessary to develop criterion for acceptable thermal comfort, calculate the mean radiant temperature, calculate interior surface temperatures, and calculate view factors to the interior surfaces.

For the purposes of this experiment, acceptable thermal comfort is achieved when the operative temperature (t_o) equals 21 °C. The operative temperature is calculated as the arithmetic mean of the indoor air temperature (t_a) and the mean radiant temperature (\bar{t}_r). This assumption is justified when the indoor air velocity is below 0.2 m/s (ASHRAE 2020a). In an effort to simplify the model, the indoor air temperature is assumed to be 21 °C at all times and at all locations in the suite.

The mean radiant temperature is calculated as the mean values of the surrounding surface temperatures, weighted by the respective view factors as per Equation 1 (ASHRAE 2021).

$$\bar{T}_r = \sqrt[4]{T_1^4 F_{p-1} + T_2^4 F_{p-2} + \dots + T_N^4 F_{p-N}}$$

where T_N is the surface temperature of the N-th surface, and F_{p-N} is the view factor between a person and surface N. The model calculates the mean radiant temperature with respect to 3 surfaces: the window, the opaque exterior wall and the radiant ceiling panel. View factors to these surfaces are calculated analytically using the solid angle formulas in (Tredre 1964). The remaining indoor surfaces such as the floor, ceiling and interior walls, are assumed to have the same surface temperature of 21 °C. Thus, their collective view factor can be established indirectly knowing that the sum of all the view factors is unity (ASHRAE 2021).

The interior surface temperature of opaque exterior walls is calculated using Equation 2, where ΔT is the indoor-outdoor temperature difference, U is the overall air-to-air U-value of the wall, and h_i is its indoor surface heat transfer coefficient. For this experiment, a standard indoor surface heat transfer coefficient of 8.3 W/m²K is assumed (ASHRAE 2021). The outdoor air temperature is read from the CWEC file.

$$T_{wall} = T_i - \frac{U \times \Delta T}{h_i}$$

The model accounts for the impact of solar radiation on the temperature of the window. While numerical models exist for accurately solving the heat balance of multi-pane windows, these can be difficult to implement and require detailed information about environmental conditions, gas fills, etc. (Curcija, et al. 2018). Instead, the present experiment opts

for a simplified approach which exploits the relationship between $SHGC$ and T_{sol} – two readily available window properties (Huizenga, et al. 2005). The difference between $SHGC$ and T_{sol} is $SHGC_{indirect}$ which represents the indirect flux of solar radiation released indoors through re-radiation and convection (Equation 3).

$$SHGC_{indirect} = SHGC - T_{sol}$$

Thus, the product of Q_{solar} and $SHGC_{indirect}$ is effectively an indoor surface heat transfer coefficient isolating for the effects of solar radiation. The solar-elevated window surface temperature can be approximated using Equation 4 (Huizenga, et al. 2005).

$$T_{window} = \frac{Q_{solar} \times SHGC_{indirect}}{h_i} + T_i$$

Q_{solar} is calculated using pvlib and values of Direct Normal Irradiance (DNI), Global Horizontal Irradiance (GHI) and Diffuse Horizontal Irradiance (DHI) from the CWEC file.

The final piece of information needed is the surface temperature (t_p) of the radiant ceiling panel. Since this is intended to vary to achieve an operative temperature of 21 °C, the required surface temperature is calculated by rearranging Equation 1. The radiant heat output of the panel, in W/m², is determined using Equation 5 (ASHRAE 2020b).

$$q_r = 5 \times 10^{-8} [(t_p + 273.15)^4 - (AUST + 273.15)^4]$$

where $AUST$ is the area-weighted temperature of all indoor surfaces excluding the radiant panel itself.

Results

The view factors between the occupant and each of the surfaces is shown in Table 2. The largest view factor was to the ceiling, floor and interior walls (“other interior surfaces”). The second largest was to the window. The radiant panel had a very small view factor (1.5 - 2.25%). Window view factors were larger with 80% WWR facades as compared to 40% WWR facades, but not linearly so (double the WWR did not result in double the view factor).

	40% WWR	80% WWR
Exterior wall	0.0543	0.0129
Window	0.0978	0.1392
Radiant ceiling panel	0.015	0.0225
Other interior surfaces	0.8329	0.8254

Table 2 – View factors from the occupant location.

The annual total heating energy demand associated with the facades is shown in Figure 2. Low Performance facades required significantly more heating energy than High Performance facades. For example, the west-facing 40% WWR Low Performance facade required 1810 kWh per year, whereas its High Performance counterpart required only 750 kWh per year (a 60% energy savings). There

was also a clear distinction between 40% WWR and 80% WWR facades, with the latter requiring approximately 85% more energy. South-facing suites consistently required the least energy and north-facing suites the most, but the impact of orientation was generally small (less than 500 kWh per year maximum deviation).



Figure 2 – Annual total heating energy demand (all facades).

Figure 3 shows the monthly total heating energy demand associated with the north-facing 80% WWR facades. The absolute energy savings of the Average and High performance facades was most evident from November to March, when the indoor-outdoor temperature difference was greatest in the Toronto weather file. Figure 4

shows the hourly heating energy demand during an especially cold week (December 13-24, 2004). At 4:00 AM on December 20, the outdoor air temperature plummeted to -24 °C triggering a peak heating demand of 1.5 kW, 1.0 kW and 0.6 kW for the Low, Average and High Performance facades respectively.

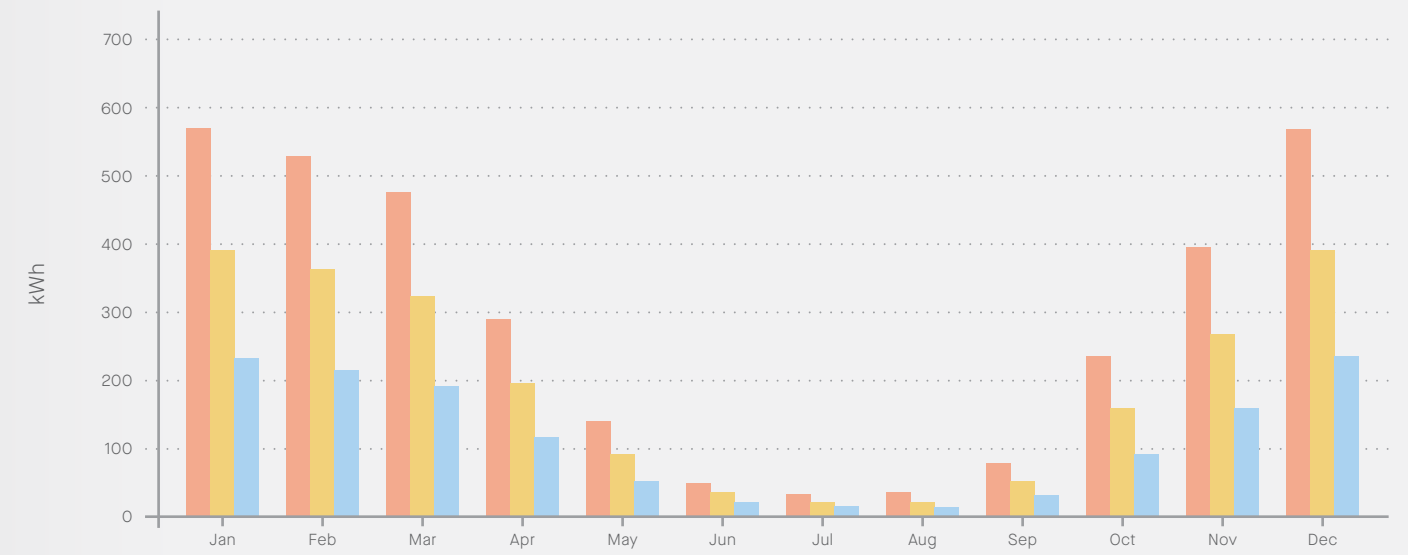


Figure 3 – Monthly total heating energy demand (north-facing 80% WWR facades).

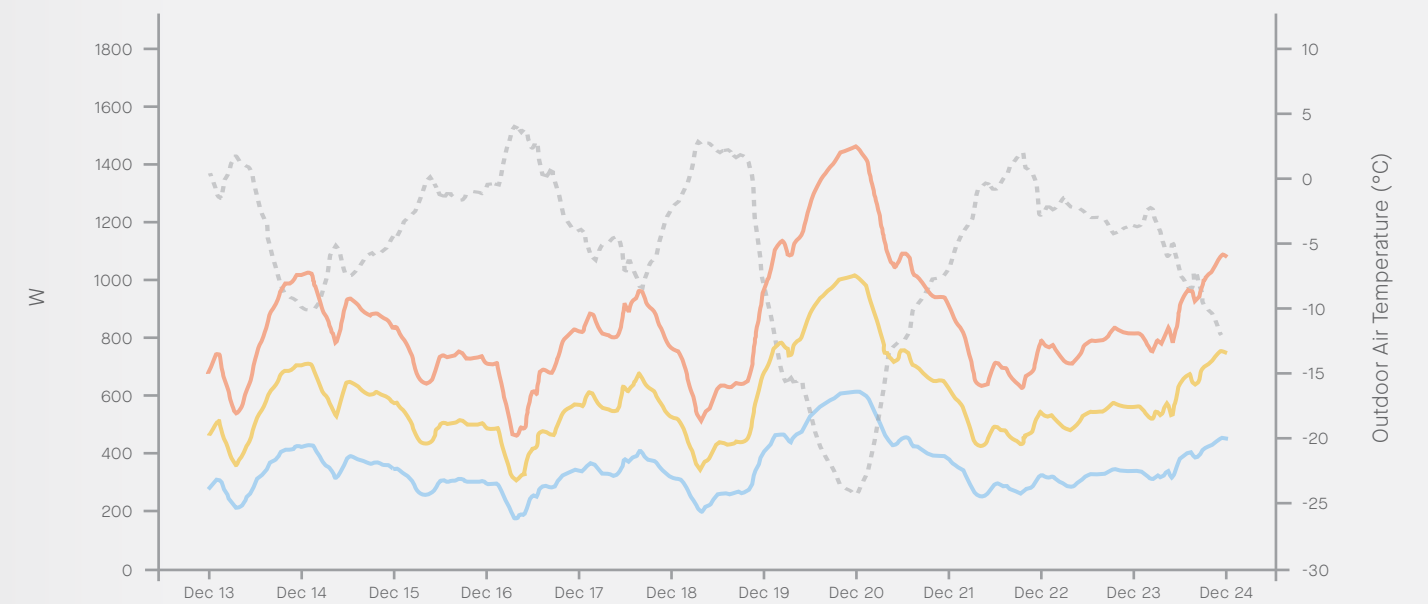
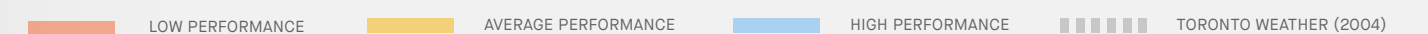


Figure 4 – Hourly heating energy demand from December 13-24, 2004 at Toronto International Airport (north-facing 80% WWR facades).



A summary of the best performing facades is shown in Table 3. The lowest annual heating energy required was 700 kWh from the south-facing 40% WWR High Performance facade. For perspective, if the residential suite had a floor area of 49 m², this would amount to a TEDI (thermal energy demand intensity) of 14 kWh/m²year, assuming the radiant panel was the sole heating equipment in the space.

	Annual heating energy (kWh)	Peak heating power (W)	Max radiant panel temperature (°C)
S_40_High Performance	700	347	53
E_40_High Performance	736	347	53
W_40_High Performance	749	347	53
N_40_High Performance	779	347	53
S_40_Average Performance	1169	563	69
S_80_High Performance	1221	612	49
E_40_Average Performance	1225	563	69
W_40_Average Performance	1245	563	69
E_80_High Performance	1286	612	49
N_40_Average Performance	1291	563	69

Table 3 – The 10 best performing facades in terms of annual heating energy demand.

Discussion

The experiment demonstrated the expected relationships between facade thermal performance and the heating energy delivered to the suite. Facades with low overall U-values and low WWRs required significantly less energy than poorly insulated facades with high WWRs. Thus, it is shown how thermal comfort and energy quantities can be used to analyze facade performance and help build an argument for higher performance facades.

Further analysis of the results revealed intricacies unique to the modelling methodology. For example, Table 1 reveals that the occupant’s view factor to the window does not increase linearly with the WWR. This can be attributed to the geometric arrangement of the experiment, which places the occupant perpendicular to the midpoint of the window. As a result, increases to the window width (WWR) occur increasingly far away from the occupant and thus have a diminishing effect on window view factor. This implies that vastly different results could be obtained by assuming a different occupant location or by introducing multiple windows. This may have special implications for dynamic facades or dynamic terminal equipment which is sensitive to occupancy.

Suite orientation had a consistent but minor impact on the annual heating energy demand. This suggests that strategies which bias more glazing towards south elevations may have limited benefit in the Toronto context. However, it should be noted that this experiment did not

consider solar radiation transmitted through the window which lands directly on the occupant or is reflected towards the occupant. Previous studies have shown that these fluxes can elevate the effective mean radiant temperature significantly (Arens, et al. 2015). Thus, it is likely the present study underestimates the differences between facade orientations.

A limitation of the model is apparent in the peak heating demands reported in Figure 4. These values seem low considering the extremity of the outdoor condition (a standard electric baseboard heater could produce enough heat for the Low Performance facade). One explanation is the static assumption of 21 °C indoor air. The model does not consider how this air temperature is achieved in -24 °C weather because it focusses on radiative heat transfer at a limited collection of surfaces. A future study could expand the model to include convective heat fluxes.

Another limitation of the model is the narrow definition of thermal comfort used. Operative temperature alone does not characterize local discomforts such as downdraft and radiant asymmetry. The latter type of discomfort is especially relevant because it may limit the maximum temperature of the radiant ceiling panel. In this case, there may arise situations where achieving local and global thermal comfort simultaneously is impossible. Future work could evaluate such situations by including radiant asymmetry in the model.



Residential suite with fully glazed curtain wall façade.

Conclusion

As high performance building design increasingly places value on the role of envelopes, it is useful for architects to be able to understand the performance implications of facade configurations at an early stage of design. This paper focussed on the thermal comfort and heating energy demand implications of facades. A Python model for assessing both these factors simultaneously was developed. The model isolates the perimeter heating energy required to maintain an operative temperature at an exact occupant location. A demonstration of the model showed the expected relationships between the inputs of WWR, U-value, SHGC and orientation; and the

outputs of heating energy (kWh) and radiant panel temperature (°C). Using the example of a typical MURB in Toronto, it was shown that a unit with a High Performance facade would require 60% less perimeter heating energy than the same unit with a Low Performance facade. Overall, the model was shown to be effective at assessing the performance of facades, and useful for building an argument for higher performance facades. However, several areas for future improvement were identified, such as the consideration of convective heat transfer, transmitted solar radiation and radiant asymmetry.

References

- Arens, Edward, Tyler Hoyt, Xin Zhou, Li Huang, Hui Zhang, and Stefano Schiavon. 2015. "Modeling the comfort effects of short-wave solar radiation indoors." *Building and Environment* 3-9.
- ASHRAE. 2020a. *ANSI/ASHRAE Standard 55-2020: Thermal Environmental Conditions for Human Occupancy*. ASHRAE.
- ASHRAE. 2021. *ASHRAE Handbook—Fundamentals*. ASHRAE.
- ASHRAE. 2020b. *ASHRAE Handbook—HVAC Systems and Equipment*. ASHRAE.
- Berardi, Umberto, and Shahrzad Soudian. 2019. "Experimental investigation of latent heat thermal energy storage using PCMs with different melting temperatures for building retrofit." *Energy & Buildings* 185: 180-195.
- Berglund, Larry G., Hiroshi Yoshino, and Satoru Kuno. 1997. "Comfort near cold perimeter walls through radiant ceiling panel and other compensation methods." *IAQ 1997 -- Design, Construction, and Operation of Healthy Buildings: Solutions to Global and Regional Concerns*. ASHRAE. 210-216.
- Curcija, Charlie, Simon Vidanovic, Robert Hart, Jacob Jonsson, and Robin Mitchell. 2018. *Window Technical Documentation*. Windows and Envelope Materials Group, Berkeley: Lawrence Berkeley National Laboratory.
- Environment Climate Change Canada. 2020. *CWEEDS/CWEC/TDY Files – 2020 Release*. Engineering Climate Services Unit, Meteorological Service of Canada, Toronto: Environment Climate Change Canada.
- Holmgren, William F., Clifford W. Hansen, and Mark A. Mikofski. 2018. "pvlib python: a python package for modeling solar energy systems." *Journal of Open Source Software* 3 (29): 884.
- Hoyt, Tyler. 2016. CBE MRT tool: *Online user guide*. Accessed September 28, 2021. <https://github.com/CenterForTheBuiltEnvironment/mrt>.
- Huizenga, Charlie, Hui Zhang, Pieter Mattelaer, Tiefeng Yu, Edward Arens, and Peter Lyons. 2005. *Window Performance for Human Thermal Comfort - Final Report*. Presentation, Berkeley: Center for the Built Environment.
- Menchaca-Brandan, M. Alejandra, Vera Baranova, Lynn Petermann, Stephanie Koltun, and Christopher Mackey. 2017. "Glazing and Winter Comfort Part 1: An Accessible Web Tool for Early Design Decision-Making." *Proceedings of the 15th IBPSA Conference*. San Francisco: IBPSA. 2449-2456.
- Ozkan, Aylin, Ted Kesik, A. Zerrin Yilmaz, and William O'Brien. 2018. "Development and visualization of time-based building energy performance." *Building Research & Innovation*.
- Sadeghipour Roudsari, Mostapha, and Michelle Pak. 2013. "Ladybug: a parametric environmental plugin for Grasshopper to help designers create an environmentally-conscious design." *Proceedings of the 13th International IBPSA Conference*. Lyon (France): IBPSA. 25-30.
- Tartarini, Federico, and Stefano Schiavon. 2020. "pythermalcomfort: A Python package for thermal comfort research." *SoftwareX* 12: 100578.
- Tredre, Barbara E. 1964. "Assessment of mean radiant temperature in indoor environments." *British Journal of Industrial Medicine* 22: 58-66.

KPMB LAB